JCAMECH

Vol. 49, No. 1, June 2018, pp 27-36
DOI: 10.22059/JCAMECH.2017.238716.169

Dynamics of nonlinear rectangular plates subjected to an orbiting mass based on shear deformation plate theory

Reza Javidi, Mahdi Moghimi Zand * *and Kia Dastani*

Small Medical Devices, Bio-MEMS & LoC Lab, School of Mechanical Engineering, College of Engineering, University of Tehran, Tehran, Iran

ARTICLE INFO

Article history:
Received: 27 July 2017
Accepted: 30 August 2017

Keywords:
Moving load
Nonlinear analysis
Plate vibration
Finite element method

ABSTRACT

In this paper, transverse and longitudinal vibration of nonlinear plate under exciting of orbiting mass is considered based on first-order shear deformation theory. The nonlinear governing equation of motion are discretized by the finite element method in combination with Newmark's time integration scheme under von Karman strain-displacement assumptions. For validation of method and formulation of solution, a simply supported beam-plate under a moving force is considered and compared with existing results in the literature. The effects of nonlinearity, mass ratios, different geometric parameters, orbiting radius and angular velocity on dynamic response of plate are studied. This study presents the importance of nonlinear analysis of rectangular plate under orbiting mass due to large deformation.

1. Introduction

Interaction between moving objects and flexible structures, according to its importance, have attracted an extensive interest in the fields of mechanical and civil engineering. The significance of the topic increasingly enhanced with technology improvement and finding new applications for different structures, e.g. bridges, multistory parking lots, high speed precision machineries, hard disk memories, wood saws, ceiling mounted cranes, and almost every structure with moving parts. Due to the fact, several researchers have studied various aspects of this issue. A comprehensive study on several simple moving load problems and their analytical solutions has been provided by Fryba [1]. Ahmadian et al. [2] have studied the dynamic behavior of Timoshenko and Euler-Bernoulli simply supported beams carrying non uniform distributed moving mass using the mode summation method. Andi et al. [3] developed a closed form solution for uniformly distributed moving masses on rectangular plate with general boundary conditioned. Eftekhari et al. [4] have studied vibration of rectangular plates under accelerated moving mass via mixed application of the Ritz method, the Differential Quadrature method, and the Integral Quadrature method. Hassanabadi et al. [5] have investigated transverse vibration of a thin rectangular plate excited by a moving oscillator along an arbitrary trajectory using the Eigen function expansion method. Vibration analysis of a rectangular plate subjected to a moving distributed load, considering the effects of inertia force, Coriolis force and centrifugal force has been performed by Wu [6]. Cifuentes and Lalapet [7] have used an adaptive mesh to study the vibration of a rectangular thin plate carrying an orbiting load utilizing finite element method. Dynamic response of the rectangular plate undergoing of a traveling point mass with combined finite element which allows for the presence of inertial effects of moving mass is provided by Esen [8]. Shahdnam et al. [9] presented a numerical-analytical method which is simply applicable in all boundary conditions for analysis of transverse vibration of nonlinear thin plates. Rofooei et al. studied the vibration of a simply supported plate carrying traveling mass, adopting a number of uniformly distributed piezoelectric patches and presented the circular and rectilinear trajectories of the traveling load in detail [10]. An adaptive mesh based on finite element method, as well as the perturbation method, is used for analysis of vibration of mindlin plates undergoing traversing loads by [11]. Takabatake [12] has provided a simplified analytical method for evaluating the transverse vibration of a rectangular plate with traveling load and stepped thickness. Gbadeyan and Oni [13] have obtained some analytical results to study vibration behavior of plate subjected moving load which is based on the modified generalized finite integral transform, the expression of the Dirac delta function as a Fourier Cosine series, and the use of the modified Struble's asymptotic method. Sofi [14] has investigated the nonlinear in-plane dynamics of inclined cables subjected to a moving oscillators with varying velocity. A semi-analytical method has been employed to solve nonlinear rectangular plate equation traveled by a moving load as well as an equivalent concentrated force with variable velocity by Mamandi et al. [15]. Significant and considerable books for analytical and numerical solution and analysis of dynamic response of structures subjected to moving load can be found in references [16-42].

* Corresponding author. Tel.: +98-21-61114807; fax: +98-21-88013029;
e-mail: mahdimoghimi@ut.ac.ir

Most of the reviewed articles deal with the linear dynamic behaviors of structures under moving load whereas in reality such systems naturally have nonlinear behavior. Especially when the plate exposed large deflection without exceed the stress failure criteria, the nonlinear parts in the strain-displacement relations cannot be ignored. In thick plate which its thickness is considerable with other dimensions cannot be neglected the deformation caused by shear. In this article, the dynamic response of thick rectangular plate that a concentrated mass travels with constant angular velocity in circular trajectory is obtained by considering the geometrically nonlinear effects. The nonlinear governing coupled equations of motion of elements are solved with the finite element method as an effective numerical method for the vibration analysis and suitable for all variants of classical boundary conditions. The approach utilizes first order shear deformation plate theory (FSDT). Inertia force, Coriolis force and centrifugal force considered in this study. The effects of plate aspect ratio, moving-mass speed and mass ratio on the nonlinear dynamic response of thick plate carrying moving mass are investigated and compared the results with related linear problem

2. Problem Formulation

A uniform undamped (FSDT) rectangular plate with length L_x , width L_y ,thickness h , density ρ , mass per unit area μ , modulus of elasticity E , Poisson's ratio ν and flexural rigidity $D = Eh^3 \big/ \left(12\left(1-\nu^2\right)\right)$ under the action of concentrated moving load traveling along an arbitrary trajectory with variable velocity, as shown as figure 1, is considered at first. Then the time-dependent function of a circular path on a square plate determined. The most important assumption of FSDT plate is that there is a linear variation of displacement across the plate thickness but that the plate thickness does not change during deformation. In this study assumes that the moving mass is always in contact with the plate surface under it. The plate assumes thick with large deflection according to first shear deformation theory.

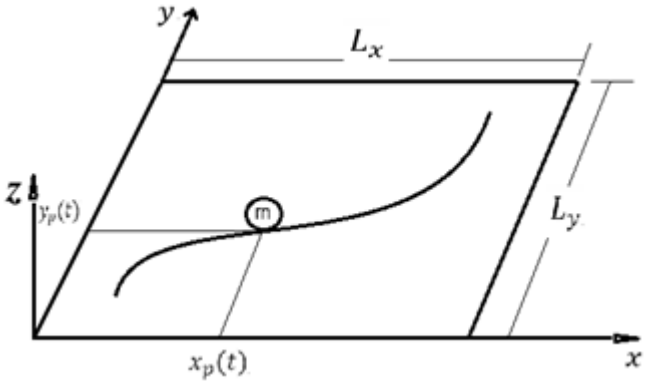

Figure. 1: A mass moving along arbitrary trajectory on the surface of rectangular plate.

Based on first shear deformation theory of plate, the displacement field can be expressed in the form [16]:

$$\begin{aligned} u(x,y,z) &= u_0(x,y) + z\phi_x(x,y) \\ v(x,y,z) &= v_0(x,y) + z\phi_y(x,y) \\ w(x,y,z) &= w_0(x,y) \end{aligned} \tag{1}$$

where (u,v,w) are the time dependent displacement in the x, y and z-axes, and ϕ_x and ϕ_y are the rotations of a transverse normal about the y and x-axes, respectively. According to the von-Karman nonlinear associated with the displacement field (Eq. 1), the strain components are defined as [16]:

$$\begin{aligned} \varepsilon_{xx} &= \frac{\partial u_0}{\partial x} + \frac{1}{2}\left(\frac{\partial w_0}{\partial x}\right)^2 + z\frac{\partial \phi_x}{\partial x} \\ \varepsilon_{yy} &= \frac{\partial v_0}{\partial y} + \frac{1}{2}\left(\frac{\partial w_0}{\partial y}\right)^2 + z\frac{\partial \phi_y}{\partial y} \\ \varepsilon_{zz} &= 0 \\ \gamma_{xy} &= \left(\frac{\partial u_0}{\partial y} + \frac{\partial v_0}{\partial x} + \frac{\partial w_0}{\partial x}\frac{\partial w_0}{\partial y}\right) + z\left(\frac{\partial \phi_x}{\partial y} + \frac{\partial \phi_y}{\partial x}\right) \\ \gamma_{xz} &= \frac{\partial w_0}{\partial x} + \phi_x \\ \gamma_{yz} &= \frac{\partial w_0}{\partial y} + \phi_y \end{aligned} \tag{2}$$

Here $\frac{1}{2}\left(\frac{\partial w_0}{\partial x}\right)^2$, $\frac{1}{2}\left(\frac{\partial w_0}{\partial y}\right)^2$ and $\frac{\partial w_0}{\partial x}\frac{\partial w_0}{\partial y}$ are the von Karman nonlinear strain, which denote the stretching of a point on the plane $z=0$ Under the above assumptions and neglecting damping, the equation of motion of nonlinear isotropic plates with assuming FSDT model are given by [16]:

$$\begin{aligned} \delta u_0 &: \frac{\partial N_{xx}}{\partial x} + \frac{\partial N_{xy}}{\partial y} - I_0\frac{\partial^2 u_0}{\partial t^2} = P_x \\ \delta v_0 &: \frac{\partial N_{xy}}{\partial y} + \frac{\partial N_{yy}}{\partial y} - I_0\frac{\partial^2 v_0}{\partial t^2} = P_y \\ \delta w_0 &: \frac{\partial Q_x}{\partial x} + \frac{\partial Q_y}{\partial y} + \frac{\partial}{\partial x}\left(N_{xx}\frac{\partial w_0}{\partial x} + N_{xy}\frac{\partial w_0}{\partial y}\right) \\ &\quad + \frac{\partial}{\partial y}\left(N_{xy}\frac{\partial w_0}{\partial x} + N_{yy}\frac{\partial w_0}{\partial y}\right) - I_0\frac{\partial^2 w_0}{\partial t^2} = P_z \\ \delta\phi_x &: \frac{\partial M_{xx}}{\partial x} + \frac{\partial M_{xy}}{\partial y} - Q_x = I_2\frac{\partial^2 \phi_x}{\partial t^2} \\ \delta\phi_y &: \frac{\partial M_{xy}}{\partial x} + \frac{\partial M_{yy}}{\partial y} - Q_y = I_2\frac{\partial^2 \phi_y}{\partial t^2} \end{aligned} \tag{3}$$

Here N_{ij}, M_{ij}, Q_j, I_0 and I_2 are in-plane force resultants, moment resultants and transverse force resultants, principal inertias and rotatory inertias, respectively [16]. P_x, P_y and P_z are the in-plane force components of the contact point that caused by gravity and the vibration acceleration of the plate.

$$\begin{aligned} P_x &= \left(m_p\frac{d^2u}{dt^2}\right)\delta\left(x-x_p(t)\right)\delta\left(y-y_p(t)\right) \\ P_y &= \left(m_p\frac{d^2v}{dt^2}\right)\delta\left(x-x_p(t)\right)\delta\left(y-y_p(t)\right) \\ P_z &= -\left(m_pg - m_p\frac{d^2w}{dt^2}\right)\delta\left(x-x_p(t)\right)\delta\left(y-y_p(t)\right) \end{aligned} \tag{4}$$

Where m_p and g are the moving mass and gravitational acceleration, respectively and $\delta(x)$ is the Dirac delta-function in x-direction.

In above equations $d^2(\ )/dt^2$ can be determined from the second-order total differential of plate deflection function [1].

$$\frac{d^2}{dt^2}=\left[\begin{array}{l}\dfrac{\partial^2}{\partial x^2}\left(\dfrac{dx}{dt}\right)^2+\dfrac{\partial^2}{\partial y^2}\left(\dfrac{dy}{dt}\right)^2\\ +\dfrac{\partial^2}{\partial t^2}+2\dfrac{\partial^2}{\partial x\partial y}\left(\dfrac{dx}{dt}\right)\left(\dfrac{dy}{dt}\right)\\ +2\dfrac{\partial^2}{\partial x\partial t}\left(\dfrac{dx}{dt}\right)+2\dfrac{\partial^2}{\partial y\partial t}\left(\dfrac{dy}{dt}\right)\\ +\dfrac{\partial}{\partial x}\left(\dfrac{d^2x}{dt^2}\right)+\dfrac{\partial}{\partial y}\left(\dfrac{d^2y}{dt^2}\right)\end{array}\right]_{x=x_p(t),\,y=y_p(t)}$$

$$\begin{aligned}x_p(t)&=x_0+V_{0x}t+\frac{1}{2}a_xt^2\\ V_{px}&=\frac{dx_p}{dt}=V_{0x}+a_xt\\ \frac{d^2x_p}{dt^2}&=a_x\\ y_p(t)&=y_0+V_{0y}t+\frac{1}{2}a_yt^2\\ V_{py}&=\frac{dy_p}{dt}=V_{0y}+a_yt\\ \frac{d^2y_p}{dt^2}&=a_y\end{aligned}\qquad(5)$$

In the above equations x_0 , y_0 and V_{0x} , V_{0y} are initial positions and velocities of the moving mass at $t=0$. a_x and a_y are the acceleration vector components of moving mass in x and y directions, respectively. The path of the moving mass is defined by the parametric coordinates $\left(x_p(t),y_p(t)\right)$. As shown in figure 2, assumed that the origin of the Cartesian coordinate system of the rectangular plate is at left and down edge of plate $(x=0,y=0)$ with the upward z-axis direction. $x_p(t)$ and $y_p(t)$ are the global positions that can be described by the following equations:

$$\begin{aligned}x_p(t)&=\frac{L_x}{2}-r\cos(\omega t)\\ y_p(t)&=\frac{L_y}{2}+r\cos(\omega t)\end{aligned}\qquad(6)$$

Where r and ω are the circular path radius and the angular frequency of the orbiting mass, respectively (Figure. 2).

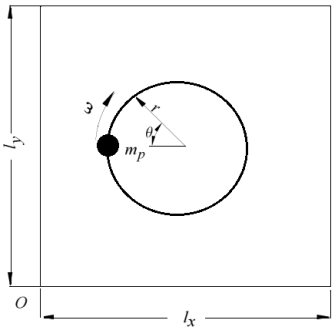

Figure. 2: The circular path of orbiting mass with radius of r and angular velocity ω

3. Finite element modeling

The weak form of the FSDT can be derived using Galerkin method. The variables $\left(u_0,v_0,w_0,\phi_x,\phi_y\right)$ can be approximated with differing degrees of Lagrange interpolation functions ψ_i as:

$$\begin{aligned}u_0(x,y)&=\sum_{j=1}^{n}U_j\psi_j(x,y)\\ v_0(x,y)&=\sum_{j=1}^{n}V_j\psi_j(x,y)\\ w_0(x,y)&=\sum_{j=1}^{n}W_j\psi_j(x,y)\\ \phi_x(x,y)&=\sum_{j=1}^{n}\Delta_j^1\psi_j(x,y)\\ \phi_y(x,y)&=\sum_{j=1}^{n}\Delta_j^2\psi_j(x,y)\end{aligned}\qquad(7)$$

Where $\left(U_j,V_j,W_j,\Delta_j^1,\Delta_j^2\right)$ are nodal values of $\left(u_0,v_0,w_0,\phi_x,\phi_y\right)$ respectively. The shape function of a nine-node rectangular element, as shown in figure 3, are:

$$\left\{\begin{array}{l}\psi_1\\ \psi_2\\ \psi_3\\ \psi_4\\ \psi_5\\ \psi_6\\ \psi_7\\ \psi_8\\ \psi_9\end{array}\right\}=\frac{1}{4}\left\{\begin{array}{l}(1-s)(1-t)(-t-s-1)+(1-s^2)(1-t^2)\\ 2(1-s^2)(1-t)-(1-s^2)(1-t^2)\\ (1+s)(1-t)(-t+s-1)+(1-s^2)(1-t^2)\\ 2(1-s)(1-t^2)-(1-s^2)(1-t^2)\\ 4(1-s^2)(1-t^2)\\ 2(1+s)(1-t^2)-(1-s^2)(1-t^2)\\ (1-s)(1+t)(t+s-1)+(1-s^2)(1-t^2)\end{array}\right\}\qquad(8)$$

In which $s=2x/a-1$ and $t=2y/b-1$ where a and b are the length and width of each rectangular plate element, respectively.

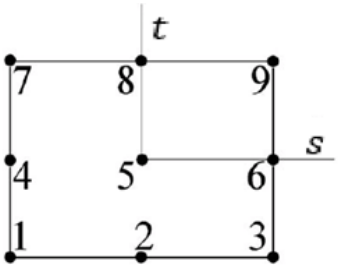

Figure. 3: Local coordinates and number of each node of the nine-node element

As shown in figure 3, the rectangular plate element is a 45-DOF plate element, therefore each node of this element is a five-degree of freedom:

$$d_i=\left\{U\ \ V\ \ W\ \ \phi_x\ \ \phi_y\right\}_i^T\qquad,i=1,2...9\qquad(9)$$

The equivalent nodal forces at each node of the nine-node element can be determined by:

$$P_i=\int_{y_1}^{y_2}\int_{x_1}^{x_2}p(x,y)\psi_i\,dx\,dy\qquad,i=1,2...9\qquad(10)$$

Hence p can be obtained by substituting Eq. (5) into Eq. (4) for each direction yield:

$$
\begin{aligned}
P_x &= m_p\left(\begin{array}{l}\dfrac{\partial^2 u}{\partial x^2}\left(\dfrac{dx}{dt}\right)^2+\dfrac{\partial^2 u}{\partial y^2}\left(\dfrac{dy}{dt}\right)^2+\dfrac{\partial^2 u}{\partial t^2}+2\dfrac{\partial^2 u}{\partial x\,\partial y}\left(\dfrac{dx}{dt}\right)\left(\dfrac{dy}{dt}\right)+2\dfrac{\partial^2 u}{\partial x\,\partial t}\left(\dfrac{dx}{dt}\right)+2\dfrac{\partial^2 u}{\partial y\,\partial t}\left(\dfrac{dy}{dt}\right)+\dfrac{\partial u}{\partial x}\left(\dfrac{d^2x}{dt^2}\right)\\ +\dfrac{\partial u}{\partial y}\left(\dfrac{d^2y}{dt^2}\right)\end{array}\right)\delta\left(x-x_p\right)\delta\left(y-y_p\right)\\
P_y &= m_p\left(\begin{array}{l}\dfrac{\partial^2 v}{\partial x^2}\left(\dfrac{dx}{dt}\right)^2+\dfrac{\partial^2 v}{\partial y^2}\left(\dfrac{dy}{dt}\right)^2+\dfrac{\partial^2 v}{\partial t^2}+2\dfrac{\partial^2 v}{\partial x\,\partial y}\left(\dfrac{dx}{dt}\right)\left(\dfrac{dy}{dt}\right)+2\dfrac{\partial^2 v}{\partial x\,\partial t}\left(\dfrac{dx}{dt}\right)+2\dfrac{\partial^2 v}{\partial y\,\partial t}\left(\dfrac{dy}{dt}\right)+\dfrac{\partial v}{\partial x}\left(\dfrac{d^2x}{dt^2}\right)\\ +\dfrac{\partial v}{\partial y}\left(\dfrac{d^2y}{dt^2}\right)\end{array}\right)\delta\left(x-x_p\right)\delta\left(y-y_p\right)\\
P_z &= m_p\left(\begin{array}{l}\dfrac{\partial^2 w}{\partial x^2}\left(\dfrac{dx}{dt}\right)^2+\dfrac{\partial^2 w}{\partial y^2}\left(\dfrac{dy}{dt}\right)^2+\dfrac{\partial^2 w}{\partial t^2}+2\dfrac{\partial^2 w}{\partial x\,\partial y}\left(\dfrac{dx}{dt}\right)\left(\dfrac{dy}{dt}\right)+2\dfrac{\partial^2 w}{\partial x\,\partial t}\left(\dfrac{dx}{dt}\right)+2\dfrac{\partial^2 w}{\partial y\,\partial t}\left(\dfrac{dy}{dt}\right)+\dfrac{\partial w}{\partial x}\left(\dfrac{d^2x}{dt^2}\right)\\ +\dfrac{\partial w}{\partial y}\left(\dfrac{d^2y}{dt^2}\right)\end{array}\right)\delta\left(x-x_p\right)\delta\left(y-y_p\right)\\
&\quad -m_p g\ \delta\left(x-x_p\right)\delta\left(y-y_p\right)
\end{aligned}
\tag{11}
$$

Writing the resulting equation by substituting Eq. (11) and (7) into Eq. (3) in the form of a matrix equation is shown as following form:

$$[m]\{\ddot{d}\}+[c]\{\dot{d}\}+[k]\{d\}=\{f\} \tag{12}$$

In which

$$
[m]=\begin{bmatrix}[m_{ij}] & [0] & [0] & [0] & [0]\\ [0] & [m_{ij}] & [0] & [0] & [0]\\ [0] & [0] & [m_{ij}] & [0] & [0]\\ [0] & [0] & [0] & [m_{ij}] & [0]\\ [0] & [0] & [0] & [0] & [m_{ij}]\end{bmatrix}
$$

$$
[c]=\begin{bmatrix}[c_{ij}] & [0] & [0] & [0] & [0]\\ [0] & [c_{ij}] & [0] & [0] & [0]\\ [0] & [0] & [c_{ij}] & [0] & [0]\\ [0] & [0] & [0] & [c_{ij}] & [0]\\ [0] & [0] & [0] & [0] & [c_{ij}]\end{bmatrix}
$$

$$
[k]=\begin{bmatrix}[k_{ij}] & [0] & [0] & [0] & [0]\\ [0] & [k_{ij}] & [0] & [0] & [0]\\ [0] & [0] & [k_{ij}] & [0] & [0]\\ [0] & [0] & [0] & [k_{ij}] & [0]\\ [0] & [0] & [0] & [0] & [k_{ij}]\end{bmatrix}
\tag{13}
$$

$$
\{f\}=\begin{Bmatrix}[m_p a_x\{\psi_i\}]\\ [m_p a_y\{\psi_i\}]\\ [m_p g\{\psi_i\}]\\ [0]\\ [0]\end{Bmatrix}
$$

Where $i=1,2...9$ and $[m]$, $[c]$ and $[k]$ are respectively the inertia force, Coriolis force and centripetal force which is presented respectively the mass, damping and stiffness matrices of moving mass element and can be expressed as:

$$
\begin{aligned}
m_{ij} &= m_p\psi_i\psi_j\\
c_{ij} &= 2m_pV_{0x}\psi_i\frac{\partial\psi_j}{\partial x}+2m_pV_{0y}\psi_i\frac{\partial\psi_j}{\partial y}\\
k_{ij} &= m_pV_{px}^2\psi_i\frac{\partial^2\psi_j}{\partial x^2}+2m_pV_{px}V_{py}\psi_i\frac{\partial^2\psi_j}{\partial x\,\partial y}\\
&\quad +m_pV_{py}^2\psi_i\frac{\partial^2\psi_j}{\partial y^2}+m_p\dot{V}_{px}\psi_i\frac{\partial\psi_j}{\partial x}+m_p\dot{V}_{py}\psi_i\frac{\partial\psi_j}{\partial y}
\end{aligned}
\tag{14}
$$

As the orbiting mass moves along the plate, the mass, damping and stiffness matrices are changed at every time step. Finite element model of damped structural system under the action of moving mass is as follows in matrices form:

$$[M]\{\ddot{\bar{d}}(t)\}+[C]\{\dot{\bar{d}}(t)\}+[K]\{\bar{d}(t)\}=\{F(t)\} \tag{15}$$

In which $[M]$, $[C]$ and $[K]$ are the overall mass, damping and stiffness matrices of structure, respectively. $\{\ddot{\bar{d}}(t)\}$, $\{\dot{\bar{d}}(t)\}$ and $\{\bar{d}(t)\}$ are, respectively, the acceleration, velocity and deflection vectors. (t) is the overall external force vector of the system. Based on FSDT, the components of plate mass, damping and stiffness matrices can be found in [16]. For considering the effect of orbiting mass, on the eth plate element at time t , the overall mass and stiffness matrices of the entire system can be calculated by adding the inertia and centripetal forces caused by moving mass element. Hence the matrices of the entire structure for all elements except for the eth element, can be written as follows:

$$
\begin{aligned}
[M] &= [m]\\
[K] &= [k]
\end{aligned}
\tag{16}
$$

And for the eth element we will have:

$$
\begin{aligned}
[M] &= [m]+[m^e]\\
[K] &= [k]+[k^e]
\end{aligned}
\tag{17}
$$

When the orbiting mass is on e[th] element, the mass and stiffness matrices caused by moving mass is added to overall property matrices of eth plate element [8]. By assembling the equations of various elements with considering the effects of moving mass, the finite element model of the total system is found. The fully discretized form of the total system is obtained using Newmark method. In this paper Newton-Raphson iteration method is used to determine deflections of central-point of plate in each step.

4. Verification of numerical solution

To verify the present method, we consider some special cases in existing literature that can be compared with our results. According to Newmark direct integration method, we used $\beta = 0.25$ and $\gamma = 0.5$ to calculate the solution of equation and verification cases. These values for γ and β are unconditionally stable for this numerical process [20].

As the first example to validate the present formulation with elimination of the nonlinear term, a simple supported beam-plate under influence of a $F = 4.4\text{N}$ moving force. This moving force travels along the centerline that is parallel to x-axes of plate with constant velocity $v = 10\text{m/s}$. The following values are utilized for the plate dimensions and material properties in literature: $L_x = 10.36\text{cm}$, $L_y = 0.635\text{cm}$, $h = 0.635\text{cm}$, $E = 206.8\text{GPa}$ and $\rho = 10686.9\text{kg/m}^3$. The existing results are compared with our results in table 1. In this table, T_f is the fundamental period and dynamic amplification factor (DAF) is the ratio of the maximum dynamic deflection to the maximum static deflection at the midpoint. The maximum deflection at the midpoint of the plate happens when the traveling time which the required time for the plate traveled by moving force (T) is near the fundamental period (T_f). Table 1 shows that our results are in a very good agreement with those found by an analytical solution for CPT plate [22] and also computed by FEM method for FSDT [43].

Table 1: Dynamic amplitude factor (DAF) versus velocity

$\frac{T_f}{T}$	v	This research	Ref. [25]	Ref. [24]	Ref. [19]
0.125	15.6	1.0623	1.042	1.063	1.025
0.25	31.2	1.1302	1.082	1.151	1.121
0.5	62.4	1.275	1.266	1.281	1.258
0.75	93.6	1.5882	-----	1.586	1.572
1	124.8	1.7053	1.662	1.704	1.701
1.25	156	1.7272	-----	1.727	1.719
2	250	1.5248	1.518	1.542	1.548

5. Results and discussion

This section elaborates the effects of large deformation and also variations of different geometrical parameters on the vibrations of the square plate under the action of orbiting mass. It is assumed that the load rotates on the circle of radius r centered at the center of the FSDT plate with a constant angular velocity ω (see figure 2). The boundary conditions of the plate are simply supported on each edge. Different properties of plate in all cases are considered as follows: $L_x = 2\text{m}$, $L_y = 2\text{m}$, $E = 200\text{GPa}$, $g = 9.81\text{m/s}^2$ and $\upsilon = 0.3$. The convergence study against the different finite element mesh for the nonlinear static analysis of the system under different values of uniform distributed load has been performed in Table 2. This table shows the center deflections of the plate that compared with those found by Reddy [16]. The convergence study for the nonlinear dynamic response of plate under an orbiting mass for different numbers of mesh elements are shown in Fig. 4. It can be seen that a finite element mesh is adequate to reach the acceptable results. We found that a time step size of $\Delta t = 5\times10^{-3}T$ is appropriately accurate approximation to achieve good convergence ($T = 2\pi/\omega$).

Figure 5 shows the vertical displacement of the central point of the system in one-cycle motion of orbiting mass ($m_p = 2\mu L_x L_y$) with simply supported edges for aspect ratios of $L_x/h = 40, 20, 10, 5$. The trajectory is a circle with radius $r = 0.4\text{m}$ and the angular velocity is $\omega = 150\text{rad/s}$. As seen, the dynamic deflection of mid-plane based on nonlinear FSDT is higher than that obtained by linear FSDT in most of the duration for all aspect ratios. Dynamic response of the square plate under the orbiting mass modeled by both linear and nonlinear plates are similar for high thicknesses, but by decreasing the plate thickness, the plate deflection differs from each other even more. Therefore, by decreasing the thickness of the plate, it is more important to use nonlinear theories for plates. Also, it can be seen that the nonlinear deflections have more oscillations than the linear one. By reducing the thickness of the plate, the number of oscillations in both linear and nonlinear models decrease.

Figure 6 and 7 show the vertical displacements of the midpoint as a function of dimensionless time in one rotation for different angular velocities ($\omega = 60, 90, 130, 200\ \text{rad/s}$) and mass ratios $\alpha = m_p/\left(\mu L_x L_y\right) = 0.5, 1, 2, 3$ to study the importance of mass weight and angular. These figures show that the maximum deflection of the nonlinear solution have almost smaller values rather than the linear solution.

Table 2: Nonlinear deflections of simply supported square plate under uniformly distributed static load

q (lb/in^2)	5×5[a]	7×7	9×9	11×11	13×13	Reddy, [21]
6.25	0.2794(3)[b]	0.2809(3)	0.2816(3)	0.282(3)	0.2821(3)	0.278
12.5	0.4609(4)	0.4625(4)	0.4632(4)	0.4635(4)	0.4637(4)	0.4619
25	0.685(5)	0.6863(5)	0.6868(5)	0.687(5)	0.6872(5)	0.6902
50	0.9479(6)	0.9482(6)	0.9485(6)	0.9486(6)	0.9487(6)	0.957
75	1.1218(7)	1.1218(7)	1.1219(7)	1.122(7)	1.1221(7)	1.133
100	1.2562(8)	1.2559(8)	1.2559(8)	1.256(8)	1.256(8)	1.2686

[a] The number of elements along x and y-direction, respectively.
[b] The number of iterations.

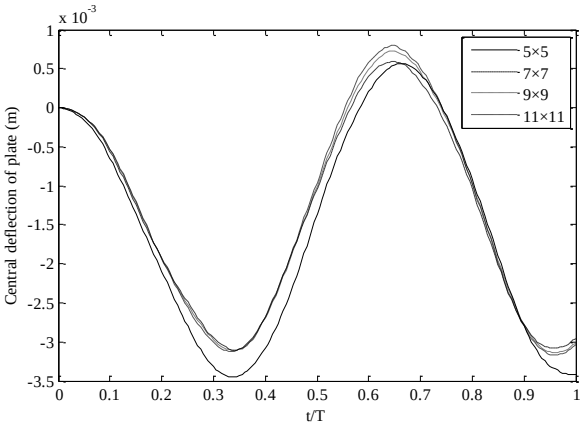

Figure 4: Midpoint deflection of plate for different number of mesh elements.

As can be seen in figure 6, for mass ratios $\alpha = 0.5, 2, 3$ the maximum deflection of the linear solution occurs at $\omega = 90\text{rad/s}$. For mass ratio of $\alpha = 1$ the maximum deflection of the linear plate occurs at $\omega = 130\text{rad/s}$. But from figure 7, it is noticed that for mass ratios of $\alpha = 0.5, 1, 2$ the maximum vertical displacements of the nonlinear solution happens at $\omega = 200\text{rad/s}$.

For mass ratio $\alpha = 3$ the maximum deflection happens at $\omega = 90\text{rad/s}$. Figure 6 and 7 shows that the significant of nonlinear analysis of the plate under heavy load. From figure 6 and 7, it can be found that the maximum vertical displacements of linear or nonlinear plate models, for an angular velocity which is reliable for a mass ratio will not necessarily be reliable for another mass ratio.

Another important parameter which influences the dynamic responses of plate under moving mass $m_p = 2\mu L_x L_y$ is the radius of orbiting trajectory, as shown in figure 8.

(a)

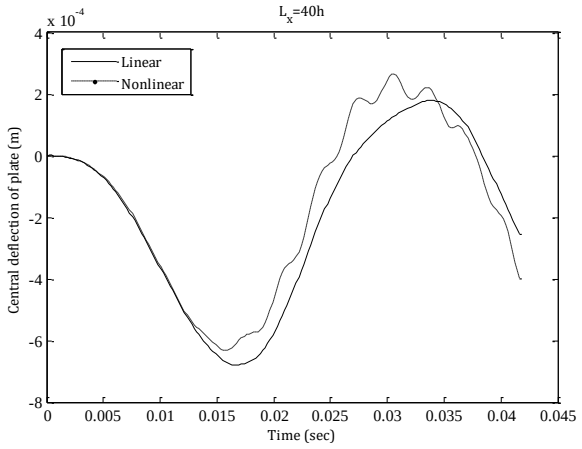

(b)

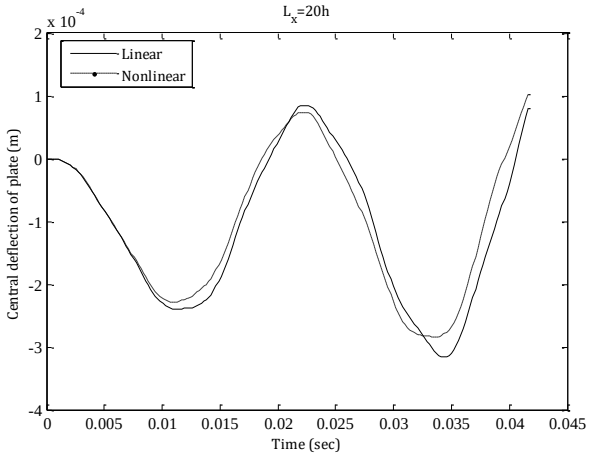

(c)

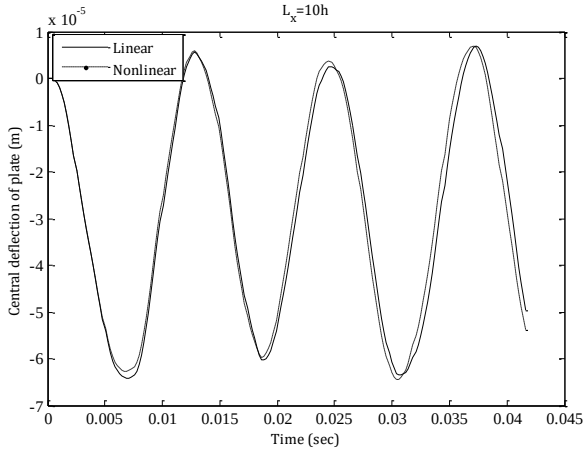

(d)

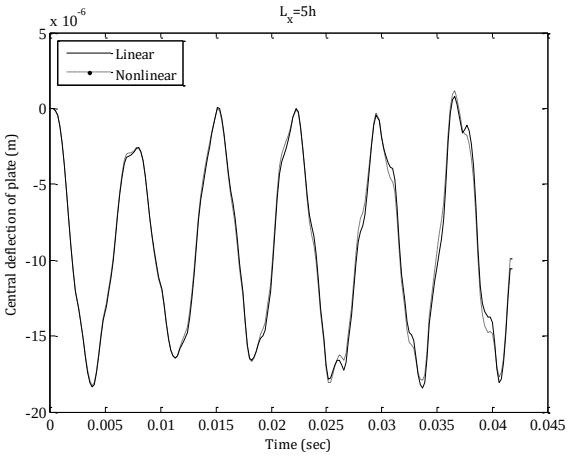

Figure 5: Dynamic vertical displacement of the central point of simply supported plate for linear and nonlinear solution versus time under the action of orbiting mass of $\alpha = 2$, at a rotation velocity of $\omega = 150\text{rad/s}$ and $r = 0.4\text{m}$ with different aspect ratios; **a)** $\frac{L_x}{h} = 40$, **b)** $\frac{L_x}{h} = 20$, **c)** $\frac{L_x}{h} = 10$ and **d)** $\frac{L_x}{h} = 5$

In figure 8, The thickness of plate is considered to be 0.05m and the mass orbits on a circular path with $\omega = 130\text{rad/s}$ In this figure linear and nonlinear FSDT models are compared at different radiuses $r = 0.15, 0.35, 0.6 \text{ and } 0.9\text{m}$. As the radius increase, the effect of geometrical nonlinearity increases noticeably and the number of oscillations of both linear and nonlinear plate increases. As seen in this figure, the maximum vertical dynamic displacement of the plate central point based on linear theory for all cases occurs at the radiuses of $r = 0.9\text{m}$, which is very close to the edge of the plate, but the maximum deflection of mid-plate based on nonlinear for all cases in this figure occurs at the radiuses of $r = 0.15\text{m}$, which is close to central point of plate. Therefore, this figure illustrates that the effect of mid-plane stretching should be considerable assumption in this analysis.

(a)

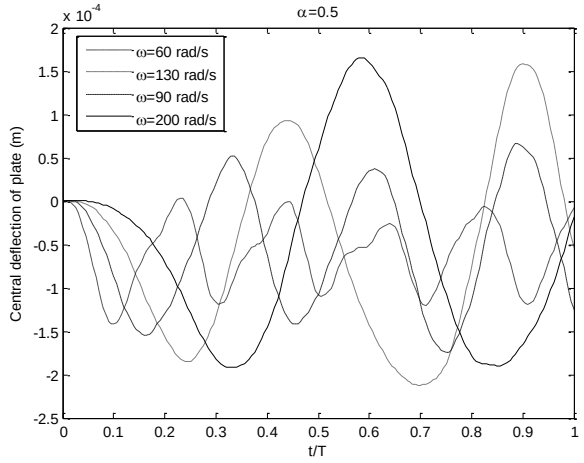

(b)

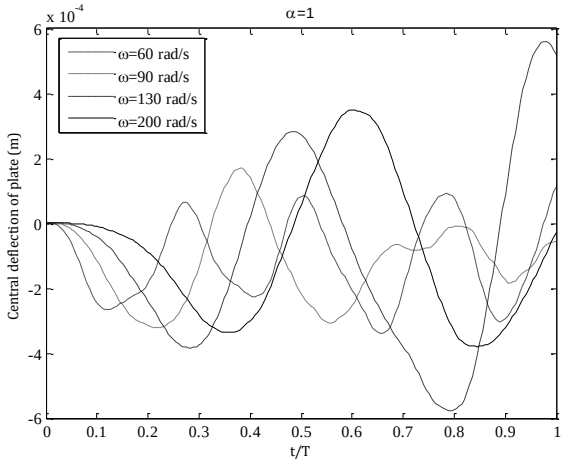

(c)

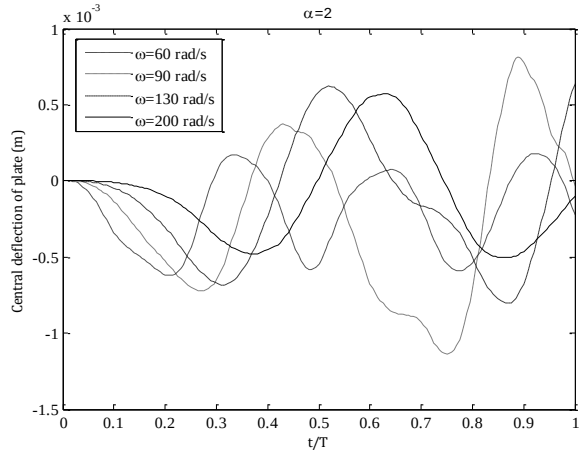

(d)

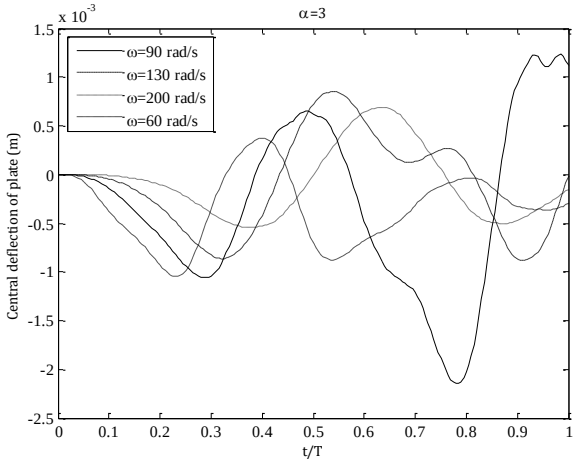

Figure 6: The effect of different angular velocity of center vertical displacement of simply supported plate with $\frac{L_x}{h} = 40$ and $r = 0.7\text{m}$ at mass ratios for linear solution; a) $\alpha = 0.5$, b) $\alpha = 1$, c) $r = \alpha = 2$ and d) $\alpha = 3$.

(a) **(b)**

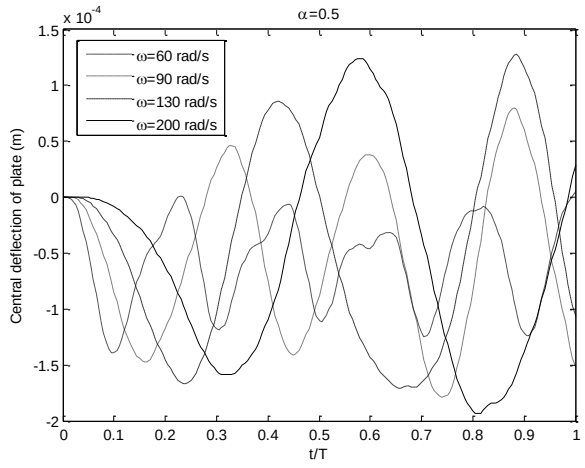

(c)

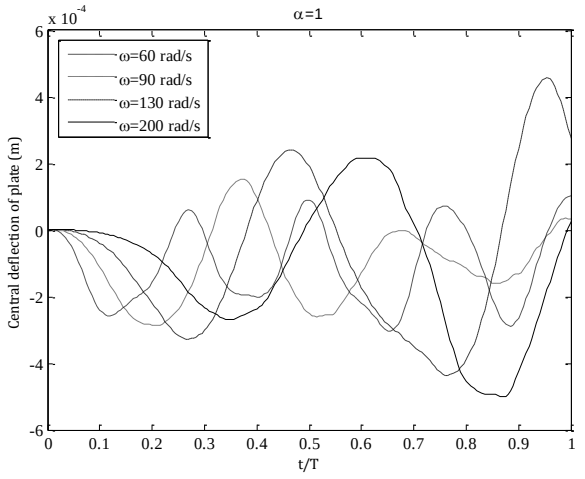

(d)

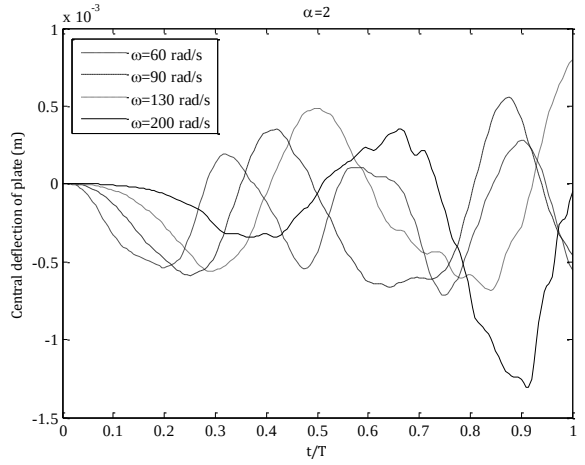

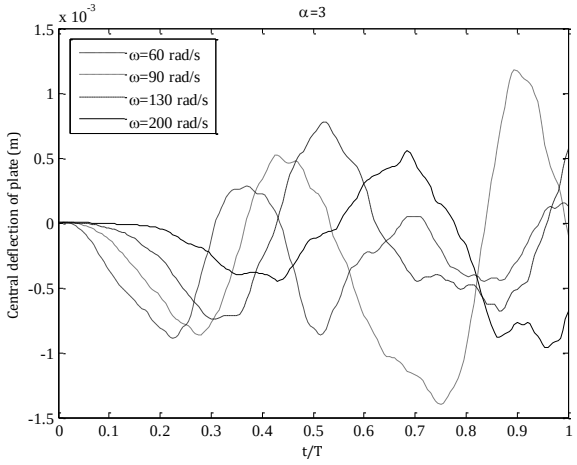

Figure 7: The effect of different angular velocity of center vertical displacement of simply supported plate with $\frac{L_x}{h}=40$ and $r=0.7\text{m}$ at mass ratios for nonlinear solution; **a)** $\alpha=0.5$, **b)** $\alpha=1$, **c)** $r=\alpha=2$ and **d)** $\alpha=3$.

(a)

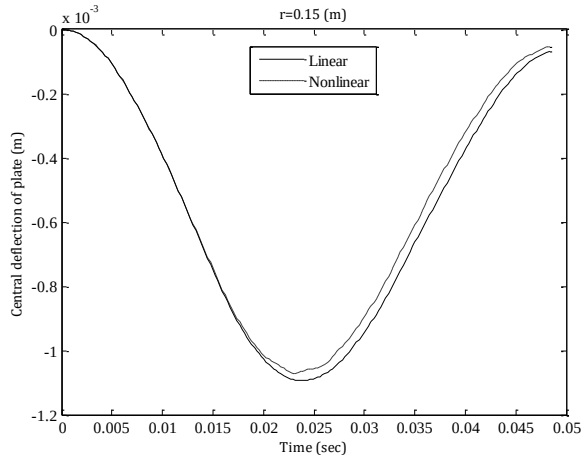

(b)

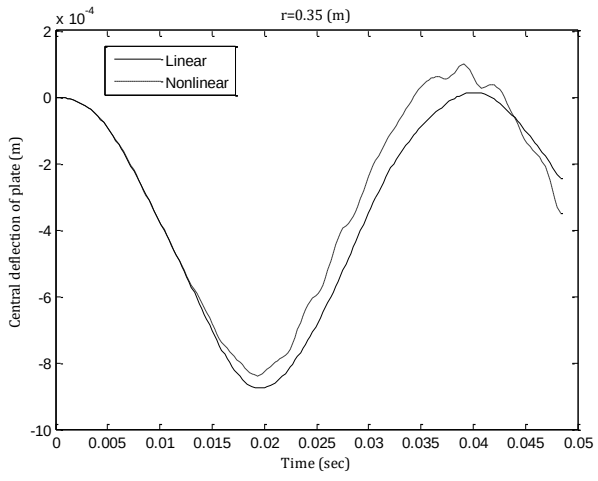

(c)

(d)

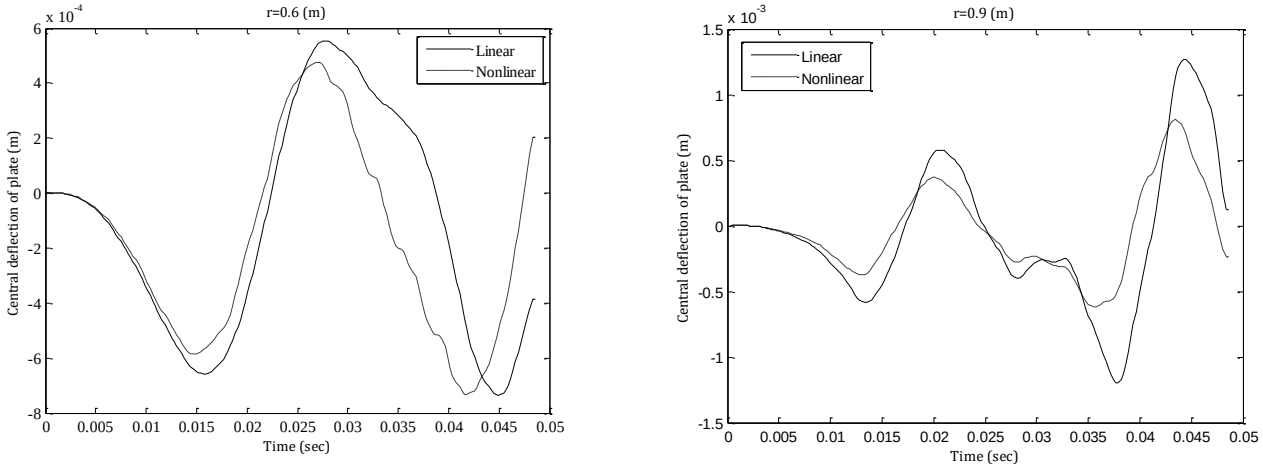

Figure 8: Dynamic response of the central point of simply supported linear and nonlinear plate versus time under the action of orbiting mass of $\alpha = 2$ at a rotation velocity of $\omega = 130\,\mathrm{rad/s}$ and $\frac{L_x}{h} = 40$ with different radius; **a)** $r = 0.15\,\mathrm{m}$, **b)** $r = 0.35\,\mathrm{m}$, **c)** $r = 0.6\,\mathrm{m}$ and d) $r = 0.9\,\mathrm{m}$.

6. Conclusion

The nonlinear dynamic behavior of undamped plate under the influence of orbiting mass has been evaluated based on first-order shear deformation plate theory using finite element method. The models have considered mid-plane stretching and all inertia effects of the mass such as the inertia force, the Coriolis and centrifugal force. The effect of angular velocity, plate thickness, mass ratio and radius of orbiting mass on the nonlinear dynamic response of square plate carrying orbiting mass is compared with the related linear problem. It was found that the maximum plate deflection in nonlinear theory was lower than linear theory in most of the time in all cases. It was observed that the effect of nonlinearity of plate in large thickness is reduced. It was shown that by increasing the radius, the difference between the nonlinear and linear vertical displacement of plate is increased. Finally, it is seen that effect of large deformation on dynamic behavior of the square plate considerably depends on the angular velocity of orbiting mass. This study reveals the significance of nonlinear analysis of plate that carried orbiting mass.

7. References

[1] L. Frýba, 2013, *Vibration of solids and structures under moving loads*, Springer Science & Business Media,

[2] M. Ahmadian, M. M. Zand, M. N. Azadani, Vibration Analysis of Timoshenko Beam Carrying Non Uniform Partially Distributed Moving Mass Using Mode Summation Method.

[3] E. A. Andi, S. T. Oni, Dynamic Analysis under Uniformly Distributed Moving Masses of Rectangular Plate with General Boundary Conditions, *Journal of Computational Engineering*, Vol. 2014, 2014.

[4] S. Eftekhari, A. Jafari, Vibration of an initially stressed rectangular plate due to an accelerated traveling mass, *Scientia Iranica*, Vol. 19, No. 5, pp. 1195-1213, 2012.

[5] M. E. Hassanabadi, J. V. Amiri, M. Davoodi, On the vibration of a thin rectangular plate carrying a moving oscillator, *Scientia Iranica. Transaction A, Civil Engineering*, Vol. 21, No. 2, pp. 284, 2014.

[6] J. J. Wu, Use of moving distributed mass element for the dynamic analysis of a flat plate undergoing a moving distributed load, *International journal for numerical methods in engineering*, Vol. 71, No. 3, pp. 347-362, 2007.

[7] A. Cifuentes, S. Lalapet, A general method to determine the dynamic response of a plate to a moving mass, *Computers & structures*, Vol. 42, No. 1, pp. 31-36, 1992.

[8] I. Esen, A new finite element for transverse vibration of rectangular thin plates under a moving mass, *Finite Elements in Analysis and Design*, Vol. 66, pp. 26-35, 2013.

[9] M. Shadnam, F. R. Rofooei, M. Mofid, B. Mehri, Periodicity in the response of nonlinear plate, under moving mass, *Thin-walled structures*, Vol. 40, No. 3, pp. 283-295, 2002.

[10] F. R. Rofooei, A. Nikkhoo, Application of active piezoelectric patches in controlling the dynamic response of a thin rectangular plate under a moving mass, *International Journal of Solids and structures*, Vol. 46, No. 11, pp. 2429-2443, 2009.

[11] A. De Faria, D. Oguamanam, Finite element analysis of the dynamic response of plates under traversing loads using adaptive meshes, *Thin-walled structures*, Vol. 42, No. 10, pp. 1481-1493, 2004.

[12] H. Takabatake, Dynamic analysis of rectangular plates with stepped thickness subjected to moving loads including additional mass, *Journal of Sound and Vibration*, Vol. 213, No. 5, pp. 829-842, 1998.

[13] J. Gbadeyan, S. Oni, Dynamic behaviour of beams and rectangular plates under moving loads, *Journal of sound and vibration*, Vol. 182, No. 5, pp. 677-695, 1995.

[14] A. Sofi, Nonlinear in-plane vibrations of inclined cables carrying moving oscillators, *Journal of sound and vibration*, Vol. 332, No. 7, pp. 1712-1724, 2013.

[15] A. Mamandi, R. Mohsenzadeh, M. H. Kargarnovin, Nonlinear dynamic analysis of a rectangular plate subjected to accelerated/decelerated moving load, *Journal of Theoretical and Applied Mechanics*, Vol. 53, No. 1, pp. 151-166, 2015.

[16] J. N. Reddy, 2014, *An Introduction to Nonlinear Finite Element Analysis: with applications to heat transfer, fluid mechanics, and solid mechanics*, OUP Oxford,

[17] M. Mohammadi, M. Ghayour, A. Farajpour, Analysis of free vibration sector plate based on elastic medium by using new version of differential quadrature method, 2011.

[18] S. K. Jalali, M. H. Naei, Large amplitude vibration analysis of graphene sheets as resonant mass sensors using mixed pseudo-spectral and integral quadrature methods, *Journal of Computational Applied Mechanics*, Vol. 45, No. 1, pp. 61-75, 2014.

[19] M. Goodarzi, M. Nikkhah Bahrami, V. Tavaf, Refined plate theory for free vibration analysis of FG nanoplates using the nonlocal continuum plate model, *Journal of Computational Applied Mechanics*, Vol. 48, No. 1, pp. 123-136, 2017.

[20] R. Szilard, 2004, *Theories and applications of plate analysis: classical numerical and engineering methods*, John Wiley & Sons,

[21] J. N. Reddy, 2002, *Energy principles and variational methods in applied mechanics*, John Wiley & Sons,

[22] L. Meirovitch, 1967, *Analytical methods in vibration*, Macmillan, New York,

[23] R. W. Clough, J. Penzien, *Dynamics of structures*, pp. 1975.

[24] H. Bachmann, W. Ammann, 1987, *Vibrations in structures: induced by man and machines*, Iabse,

[25] T. Yang, 1986, *Finite element structural analysis*, Prentice Hall,

[26] D. Yoshida, W. Weaver, Finite element analysis of beams and plates with moving loads, *Publication of International Association for Bridge and Structural Engineering*, Vol. 31, No. 1, pp. 179-195, 1971.

[27] A. Daneshmehr, A. Rajabpoor, A. Hadi, Size dependent free vibration analysis of nanoplates made of functionally graded materials based on nonlocal elasticity theory with high order theories, *International Journal of Engineering Science*, Vol. 95, pp. 23-35, 2015.

[28] M. Z. Nejad, A. Rastgoo, A. Hadi, Exact elasto-plastic analysis of rotating disks made of functionally graded materials, *International Journal of Engineering Science*, Vol. 85, pp. 47-57, 2014.

[29] M. Nejad, A. Rastgoo, A. Hadi, Effect of Exponentially-Varying Properties on Displacements and Stresses in Pressurized Functionally Graded Thick Spherical Shells with Using Iterative Technique, *Journal of Solid Mechanics Vol*, Vol. 6, No. 4, pp. 366-377, 2014.

[30] M. Z. Nejad, A. Hadi, Non-local analysis of free vibration of bi-directional functionally graded Euler–Bernoulli nano-beams, *International Journal of Engineering Science*, Vol. 105, pp. 1-11, 8//, 2016.

[31] M. Z. Nejad, A. Hadi, Eringen's non-local elasticity theory for bending analysis of bi-directional functionally graded Euler–Bernoulli nano-beams, *International Journal of Engineering Science*, Vol. 106, pp. 1-9, 9//, 2016.

[32] M. Z. Nejad, A. Hadi, A. Rastgoo, Buckling analysis of arbitrary two-directional functionally graded Euler–Bernoulli nano-beams based on nonlocal elasticity theory, *International Journal of Engineering Science*, Vol. 103, pp. 1-10, 6//, 2016.

[33] M. Hosseini, M. Shishesaz, K. N. Tahan, A. Hadi, Stress analysis of rotating nano-disks of variable thickness made of functionally graded materials, *International Journal of Engineering Science*, Vol. 109, pp. 29-53, 12//, 2016.

[34] Z. Mazarei, M. Z. Nejad, A. Hadi, Thermo-elasto-plastic analysis of thick-walled spherical pressure vessels made of functionally graded materials, *International Journal of Applied Mechanics*, Vol. 8, No. 04, pp. 1650054, 2016.

[35] M. Z. Nejad, A. Hadi, A. Farajpour, Consistent couple-stress theory for free vibration analysis of Euler-Bernoulli nano-beams made of arbitrary bi-directional functionally graded materials, *Structural Engineering and Mechanics*, Vol. 63, No. 2, pp. 161-169, 2017.

[36] M. M. Adeli, A. Hadi, M. Hosseini, H. H. Gorgani, Torsional vibration of nano-cone based on nonlocal strain gradient elasticity theory, *The European Physical Journal Plus*, Vol. 132, No. 9, pp. 393, September 18, 2017.

[37] M. Hosseini, H. H. Gorgani, M. Shishesaz, A. Hadi, Size-Dependent Stress Analysis of Single-Wall Carbon Nanotube Based on Strain Gradient Theory, *International Journal of Applied Mechanics*, Vol. 9, No. 06, pp. 1750087, 2017.

[38] M. Shishesaz, M. Hosseini, K. N. Tahan, A. Hadi, Analysis of functionally graded nanodisks under thermoelastic loading based on the strain gradient theory, *Acta Mechanica*, pp. 1-28, 2017.

[39] M. Farajpour, A. Shahidi, A. Hadi, A. Farajpour, Influence of initial edge displacement on the nonlinear vibration, electrical and magnetic instabilities of magneto-electro-elastic nanofilms, *Mechanics of Advanced Materials and Structures*, pp. 1-13, 2018.

[40] A. Afshin, M. Zamani Nejad, K. Dastani, Transient thermoelastic analysis of FGM rotating thick cylindrical pressure vessels under arbitrary boundary and initial conditions, *Journal of Computational Applied Mechanics*, Vol. 48, No. 1, pp. 15-26, 2017.

[41] M. Gharibi, M. Zamani Nejad, A. Hadi, Elastic analysis of functionally graded rotating thick cylindrical pressure vessels with exponentially-varying properties using power series method of Frobenius, *Journal of Computational Applied Mechanics*, Vol. 48, No. 1, pp. 89-98, 2017.

[42] M. Zamani Nejad, M. Jabbari, A. Hadi, A review of functionally graded thick cylindrical and conical shells, *Journal of Computational Applied Mechanics*, Vol. 48, No. 2, pp. 357-370, 2017.

[43] M. Kadivar, S. Mohebpour, Finite element dynamic analysis of unsymmetric composite laminated beams with shear effect and rotary inertia under the action of moving loads, *Finite Elements in Analysis and Design*, Vol. 29, No. 3, pp. 259-273, 1998.